

See discussions, stats, and author profiles for this publication at: <https://www.researchgate.net/publication/224543258>

Conversion of Near-Ultraviolet Radiation Into Visible and Infrared Emissions Through Energy Transfer in Yb₂O₃ Doped SrO–TiO₂–SiO₂ Glasses

ARTICLE in JOURNAL OF APPLIED PHYSICS · APRIL 2009

Impact Factor: 2.18 · DOI: 10.1063/1.3097381 · Source: IEEE Xplore

CITATIONS

10

READS

56

8 AUTHORS, INCLUDING:



Song Ye

Tongji University

62 PUBLICATIONS 1,174 CITATIONS

SEE PROFILE



Yin Liu

University of Illinois, Urbana-Champaign

20 PUBLICATIONS 333 CITATIONS

SEE PROFILE



Geng Lin

Huawei Technologies

49 PUBLICATIONS 500 CITATIONS

SEE PROFILE



Jianrong Qiu

South China University of Technology

691 PUBLICATIONS 11,253 CITATIONS

SEE PROFILE

Conversion of near-ultraviolet radiation into visible and infrared emissions through energy transfer in Yb 2 O 3 doped SrO – TiO 2 – SiO 2 glasses

Song Ye, Bin Zhu, Yin Liu, Yu Teng, Geng Lin, Gandham Lakshminarayana, Xianping Fan, and Jianrong Qiu

Citation: [Journal of Applied Physics](#) **105**, 063508 (2009); doi: 10.1063/1.3097381

View online: <http://dx.doi.org/10.1063/1.3097381>

View Table of Contents: <http://scitation.aip.org/content/aip/journal/jap/105/6?ver=pdfcov>

Published by the [AIP Publishing](#)

Articles you may be interested in

[Extraordinary infrared photoluminescence efficiency of Er 0.1 Yb 1.9 SiO 5 films on SiO 2 / Si substrates](#)
Appl. Phys. Lett. **98**, 071903 (2011); 10.1063/1.3554750

[Photoluminescence in electronic ferroelectric Er 1 x Yb x Fe 2 O 4](#)
J. Appl. Phys. **108**, 073507 (2010); 10.1063/1.3490212

[Near infrared quantum cutting in heavy Yb doped Ce 0.03 Yb 3 x Y \(2.97 3 x \) Al 5 O 12 transparent ceramics for crystalline silicon solar cells](#)
J. Appl. Phys. **107**, 043107 (2010); 10.1063/1.3298907

[Frequency upconversion luminescence from Yb + 3 – Tm + 3 codoped PbO – GeO 2 glasses containing silver nanoparticles](#)
J. Appl. Phys. **106**, 063522 (2009); 10.1063/1.3211300

[Energy transfer between silicon–oxygen-related defects and Yb 3 + in transparent glass ceramics containing Ba 2 TiSi 2 O 8 nanocrystals](#)
Appl. Phys. Lett. **93**, 181110 (2008); 10.1063/1.3021086



AIP | Journal of
Applied Physics

Journal of Applied Physics is pleased to
announce **André Anders** as its new Editor-in-Chief

Conversion of near-ultraviolet radiation into visible and infrared emissions through energy transfer in Yb₂O₃ doped SrO–TiO₂–SiO₂ glasses

Song Ye,¹ Bin Zhu,¹ Yin Liu,¹ Yu Teng,¹ Geng Lin,² Gandham Lakshminarayana,¹ Xianping Fan,¹ and Jianrong Qiu^{1,2,a)}

¹State Key Laboratory of Silicon Materials, Zhejiang University, Hangzhou 310027, China

²State Key Laboratory of High Field Laser Physics, Shanghai Institute of Optics and Fine Mechanics, Chinese Academy of Sciences, Shanghai 201800, China

(Received 10 November 2008; accepted 8 February 2009; published online 18 March 2009)

We demonstrated the conversion of near-ultraviolet radiation of 250–350 nm into visible emission of 450–600 nm and near-infrared emission of 970–1100 nm in the Yb₂O₃ doped transparent 40SrO–20TiO₂–40SiO₂ glasses. The observed broad visible emission band centered at 510 nm is associated with silicon-oxygen-related defects in the glassy matrix, and the near-infrared emission originated from the Yb³⁺ ²F_{5/2} → ²F_{7/2} transition is due to the energy transfer from silicon-oxygen-related defects to Yb³⁺. The energy transfer process was studied by both the steady state spectra and the time-resolved spectra of Yb³⁺ at 15 K. The temperature dependent energy transfer rate was calculated. The Yb₂O₃ concentration dependent energy transfer efficiency has also been evaluated, and the maximum value is 56% for 12 mol % Yb₂O₃ doped glass. © 2009 American Institute of Physics. [DOI: 10.1063/1.3097381]

I. INTRODUCTION

Considerable research has been focused on rare earth ions and transition metal ions doped glasses due to their potential applications in optical telecommunications, solid state lasers and three-dimensional full-color displays.^{1–4} Recently, these materials have also been used in photovoltaic applications to improve solar cell efficiency.^{5–7} Compared to powder samples, glasses are more suitable for solar cell owing to their high transparency to visible light and desirable mechanical and chemical properties. One of the major sources for energy losses in solar cell is due to thermalize charge carriers generated by the absorption of high-energy photons.^{8,9} Fortunately, the high-energy part of the solar spectrum can be used more efficiently by either down-conversion or photoluminescence processes. These two processes are distinguished by the quantum efficiency: the former is larger than one, while the latter is smaller than one. The infrared quantum cutting process, which converts the high-energy part of the solar spectrum into the near-infrared wavelength region that can be efficiently absorbed by the solar cell, has been reported in the glass-ceramics codoped with rare earth ions such as Tb³⁺–Yb³⁺, Tm³⁺–Yb³⁺, and Pr³⁺–Yb³⁺, in which Tb³⁺, Tm³⁺, and Pr³⁺ act as the absorption centers.^{5–7,10,11} In this work, we focused on the spectral modification through photoluminescence process to utilize the high-energy part of solar spectrum.

Previously, it was reported that the glass-ceramics containing Ba₂TiSi₂O₈ nanocrystals exhibit visible green emissions under near-ultraviolet irradiation. The origin of the visible emission was suggested to be related with the oxygen-deficient defects in TiO₅ octahedra or SiO₄ tetrahedra.^{12,13} In the 40SrO–20TiO₂–40SiO₂ glass system, we observed a simi-

lar broad emission band centered at 520 nm, which is proved to be related with the silicon-oxygen-related defects by our experiment. We demonstrated in the Yb₂O₃ doped transparent 40SrO–20TiO₂–40SiO₂ glass that an efficient visible emission occurs in the range of 450–600 nm, which is due to the silicon-oxygen-related defect absorption, and an infrared emission originates from Yb³⁺ ²F_{5/2} → ²F_{7/2} transition due to the energy transfer from the silicon-oxygen-related defects to Yb³⁺. In this system, the extraterrestrial solar irradiance of 250–350 nm is converted into the visible emission of 450–600 nm, together with the near-infrared emission of 960–1100 nm where the silicon solar cells exhibit the greatest spectral response.^{14,15} In addition to the excitation and emission spectra, Yb³⁺ luminescence decay and time-resolved emission spectra were also measured at low temperatures to further confirm the energy transfer process. Based on the measured emission lifetime of the silicon-oxygen-related defects, the temperature dependent energy transfer rate and Yb₂O₃ concentration dependent energy transfer efficiency have also been evaluated.

II. EXPERIMENTAL

Glasses with compositions of 40SrO–20TiO₂–40SiO₂–*x*Yb₂O₃ (STS) (*x*=0, 1, 1.5, 2, 4, and 8 mol %) and 45SrO–55SiO₂–*x*Yb₂O₃ (SS) (*x*=0 and 2 mol %) were synthesized by using 4N-purity grade SrCO₃, TiO₂, SiO₂, and Yb₂O₃. The raw materials were mixed homogeneously and melt at 1550 °C for STS glasses and 1650 °C for SS glasses in Pt crucibles for 2 h in air. The melts were poured onto a heated brass plate at 300 °C and then pressed to about 2 mm using another brass plate. The obtained transparent glasses were annealed at 680 °C for 2 h. X-ray diffraction profiles of the annealed glasses were recorded using a Rigaku D/MAX-RA diffractometer with Cu Kα as an incident radiation. According to x-ray diffrac-

^{a)}Author to whom correspondence should be addressed. Electronic mail: qjr@zju.edu.cn.

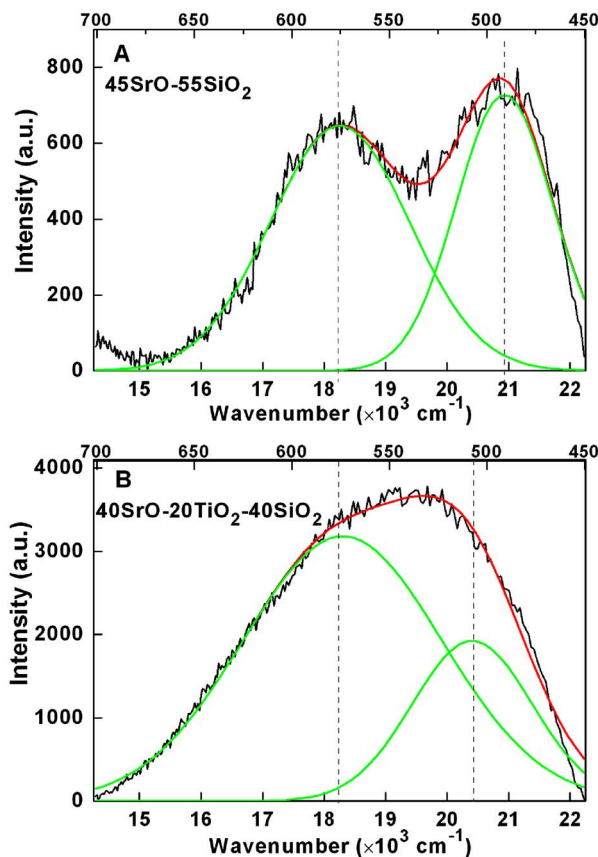


FIG. 1. (Color online) Visible emission originated from SS glass (a) and STS glass (b), respectively, excited by 320 nm. Each emission spectrum is decomposed into two Gaussian functions.

tion measurements, these glass samples are amorphous. Excitation and emission spectra, fluorescence decay curves, and time-resolved spectra in both visible and infrared regions were recorded using a FLS920 fluorescence spectrophotometer. The low temperature was obtained by ARS-2HW compressor.

III. RESULTS AND DISCUSSION

A. Visible emission originated from the silicon-oxygen-related defect in STS glass

It was reported that the glass-ceramic containing $\text{Ba}_2\text{TiSi}_2\text{O}_8$ nanocrystals (glass composition:

$\text{BaO-TiO}_2\text{-SiO}_2$) exhibits a broad green luminescence in the range of 400–600 nm with near-ultraviolet excitation. In our present work, we also observed similar visible green emission in the $40\text{SrO-20TiO}_2\text{-40SiO}_2$ glass, which corresponds to a broad excitation band in the near-ultraviolet region. However, the mechanism for this visible green emission is still not clear. It was suggested that this visible green emission is either due to the oxygen-deficient defects in TiO_5 octahedra or in SiO_4 units in the $\text{Ba}_2\text{TiSi}_2\text{O}_8$ nanocrystals.^{12,13} In order to clarify the argument, we also carried out the same measurements in the Ti^{4+} free glass samples 45SrO-55SiO_2 (SS). The emission spectra of the SS and STS glasses excited by 320 nm are illustrated in Figs. 1(A) and 1(B), respectively. The broad green emission band can still be observed in the Ti^{4+} -free glass, but the emission intensity is much lower than that in the STS glass. Each visible emission in the SS and STS glasses can be fitted by two Gaussian functions in wave numbers, which may correspond to two luminescence centers with different crystal fields. By comparing the simulated results in Figs. 1(A) and 1(B) we can observe that the two groups of Gaussian shapes hold very similar peak positions and full width at half maximum (FWHM), but different intensity ratios. Based on these experimental results, we suggest that the green emission is most likely originated from the silicon-oxygen-related defects in the SiO_4 units, as suggested by Yang *et al.*,¹⁶ yet have the indirect relationship with the Ti^{4+} ions. Concretely, the introduction of TiO_2 greatly enhanced the intensity of the green emission (also shown in Fig. 2), and altered the Gaussian peak positions and the FWHM, as well as the intensity ratio of the two Gaussian shapes.

B. Room temperature and low temperature steady spectra

The excitation and emission spectra of Yb^{3+} -free and 2 mol % Yb_2O_3 doped STS glasses are shown in Fig. 2. In the Yb^{3+} -free STS glass, a broad green emission band centered at 520 nm is observed with near-ultraviolet radiation, which corresponds to the broad excitation band in the wavelength region of 250–350 nm. Since the green emission is observed in the Yb^{3+} -free STS glass, the possible origin of cooperative de-excitation of two Yb^{3+} ions could be elimi-

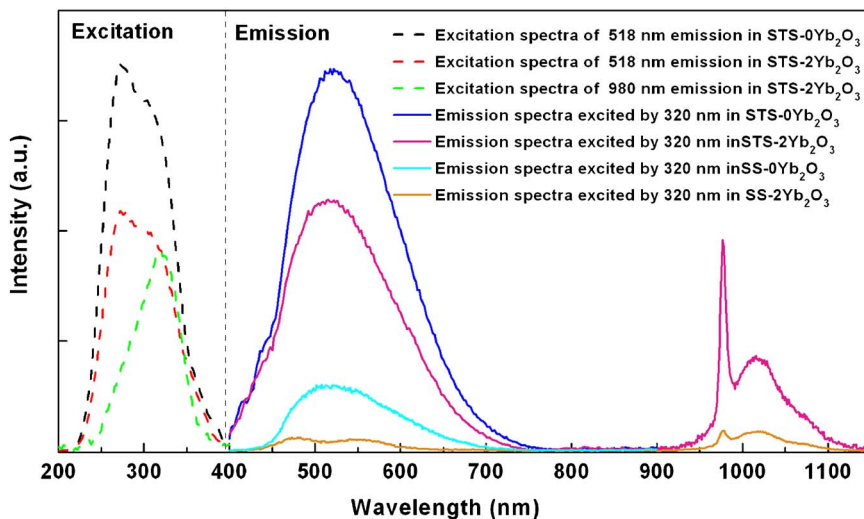


FIG. 2. (Color online) Excitation ($\lambda_{em}=520$ nm) and emission ($\lambda_{ex}=320$ nm) spectra monitored for the Yb^{3+} -free and 2 mol % Yb_2O_3 doped STS glass. The emission spectra of Yb^{3+} -free and 2 mol % Yb_2O_3 doped SS glass under 320 nm excitation are also given for comparison.

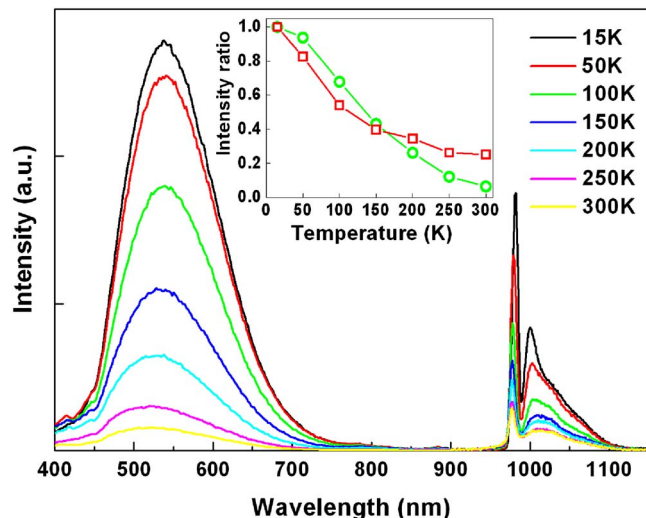


FIG. 3. (Color online) Temperature dependent emission spectra of the silicon-oxygen-related defect under 320 nm excitation. The inset shows the normalized integral intensity of visible emission (green circle) and infrared emission (red square) as a function of temperature.

nated in the Yb_2O_3 doped STS glasses. For the 2 mol % Yb_2O_3 doped STS glass, infrared emissions at 980 and 1016 nm, corresponding to the transitions from the lowest Stark level of the $\text{Yb}^{3+} {}^2\text{F}_{5/2}$ multiplet to two different Stark levels of the ${}^2\text{F}_{7/2}$ multiplet, are obtained under 320 nm excitation with an observation of decrement in the green emission intensity. The excitation spectrum of Yb^{3+} 980 nm emission overlaps well with the excitation spectrum of the green emission. This indicates the existence of energy transfer between the green emission and Yb^{3+} .⁴

The emission spectra of the Yb_2O_3 doped STS glass at different temperatures (15, 50, 100, 150, 200, 250, and 300 K, respectively) with 320 nm excitation are shown in Fig. 3. The luminescence intensities in both the visible and infrared regions decrease rapidly with increasing temperature. The decrease in emission intensity may be caused by the thermal quenching process. The normalized integral intensity versus temperature is given in the inset of Fig. 3. It is clearly shown that the intensity ratios of the infrared to visible emission increase monotonously with increasing temperature, indicating enhanced energy transfer efficiency. At 15 K, only the visible emission due to the silicon-oxygen-related defects in the STS glass and the infrared emission due to the transitions from different Stark energy levels of $\text{Yb}^{3+} {}^2\text{F}_{5/2}$ and ${}^2\text{F}_{7/2}$ manifolds are monitored under the excitation of defect absorption at 320 nm. The charge transfer luminescence of Yb^{3+} , which is characterized by the broad emission band in the visible region with two subbands separated by about $10\,000\text{ cm}^{-1}$, is not observed.¹⁷ This indicates that the infrared emission of Yb^{3+} in the range of 950–1150 nm is due to the energy transfer from the silicon-oxygen-related defect, rather than from the charge transfer state absorption. Generally, the Yb^{3+} charge transfer absorption band is located at the wavelength region shorter than 250 nm, and the quenching temperature of charge transfer luminescence is higher than 100 K in oxides.¹⁸

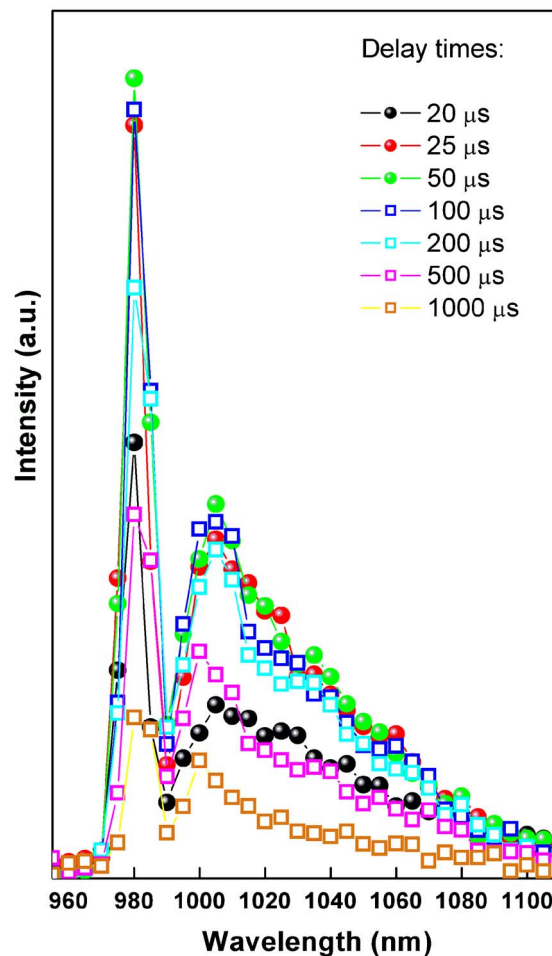


FIG. 4. (Color online) Time-resolved emission spectra of the Yb^{3+} infrared emission under 320 nm excitation at 15 K.

C. Time-resolved emission spectra at low temperature

In order to further prove the energy transfer process from the silicon-oxygen-related defects to Yb^{3+} ions, the time-resolved emission spectra in the 1 mol % Yb_2O_3 doped STS glass were recorded at 15 K with the excitation of defect absorption at 320 nm. As shown in Fig. 4, the Yb^{3+} emission intensity increases within the $50\text{ }\mu\text{s}$ delay, and then decreases when the time delay is longer than $100\text{ }\mu\text{s}$. These observations are consistent with the population and depopulation processes of $\text{Yb}^{3+} {}^2\text{F}_{5/2}$ energy level, respectively. The time-resolved fluorescence spectra monitored as a function of time after excitation by a flash light support the energy transfer model well.^{19,20}

D. Temperature dependent energy transfer rate

The energy transfer rate as a function of temperature was also evaluated. The lifetimes of silicon-oxygen-related defect emissions at different temperatures in the Yb^{3+} -free and 1 mol % Yb_2O_3 doped STS glasses are shown in Fig. 5. Due to the disordered nature of glasses, the environment around each silicon-oxygen-related defect may not be identical, resulting in site-to-site differences in the radiative and nonradiative transition probabilities of the visible emission origi-

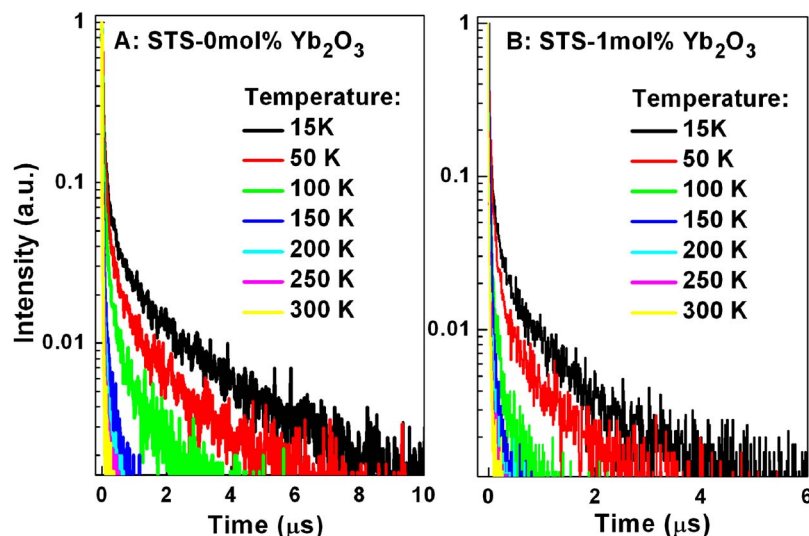


FIG. 5. (Color online) Luminescence decay curves of silicon-oxygen-related defect in Yb³⁺-free STS glass (a) and 1 mol % Yb₂O₃ doped STS glass (b), respectively, under 320 nm excitation at different temperatures.

nated from the defects. Therefore, the measured decay rate under broadband excitation (different from fluorescence line narrowing where the laser is used as the excitation source) is a superposition of contributions from individual defects.¹⁹ Since the measured decay rate is treated by ascribing the average rates to the system, the fluorescence following pulsed broadband excitation exhibits a nonsingle-exponential time dependent. That is the reason why the defects emission decays deviated from the single-exponential form in the Yb³⁺-free STS glass. As the decay of the defect shows a nonexponential characteristic, the mean decay lifetime (τ_m) is given by $\tau_m = \int_{t_0}^{\infty} I(t)/I_0 dt$, where $I(t)$ is the luminescence intensity as a function of time t , and I_0 is the maximum of $I(t)$, which occurs at the initial time t_0 . The lifetime of the silicon-oxygen-related defect decreases drastically from 140.28 to 5.74 μ s for Yb³⁺-free glass and from 59.54 to 4.38 μ s for 1 mol % Yb₂O₃ doped glass, respectively, with increasing temperature. Generally, an increase in temperature will lead to the population of higher vibrational levels, which results in a broadening of the FWHM of the emission band (as shown in Fig. 3) and a shorter lifetime due to the nonradiative transfer between vibrational levels.

The measured D - A energy transfer rate can be obtained by the following relationship:

$$W = \frac{1}{\tau_m} - \frac{1}{\tau_{m0}},$$

where τ_m and τ_{m0} are the mean fluorescence lifetime of the defect in the presence and absence of the Yb³⁺ ions, respectively. The evaluated energy rate with error bar is shown in Fig. 6. It is seen that the energy transfer rate is strongly temperature dependent, which increases rapidly with increasing temperature, indicating a photon-assistant energy transfer process.²⁰

E. Concentration dependent energy transfer efficiency

Figure 7 depicts the decay curves of the silicon-oxygen-related defects emission at 520 nm under 320 nm excitation. It is seen that the defect emission decays rapidly with increasing Yb₂O₃ concentration. This is due to the presence of Yb³⁺ as an extra decay pathway. As the decay shows nonexponential characteristic, the lifetime is also treated as a mean decay lifetime τ_m .

The energy transfer efficiency η_{ET} is defined as the ratio of donors that are depopulated by energy transfer to the acceptors over the total number of donors being excited. In our system, the silicon-oxygen-related defect acts as the donor

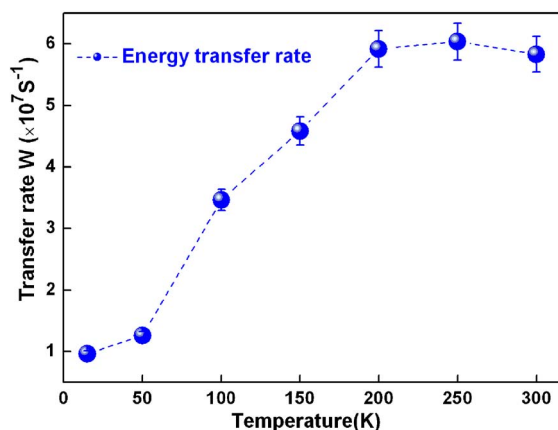


FIG. 6. (Color online) Temperature dependent energy transfer rate in the 1 mol % Yb₂O₃ doped STS glass.

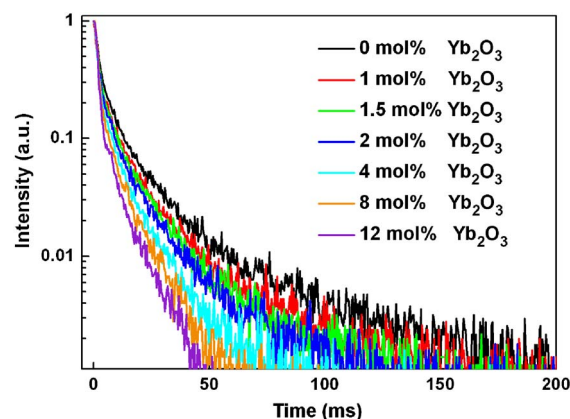


FIG. 7. (Color online) Luminescence decay curves of the defects emission at 520 nm under 320 nm excitation.

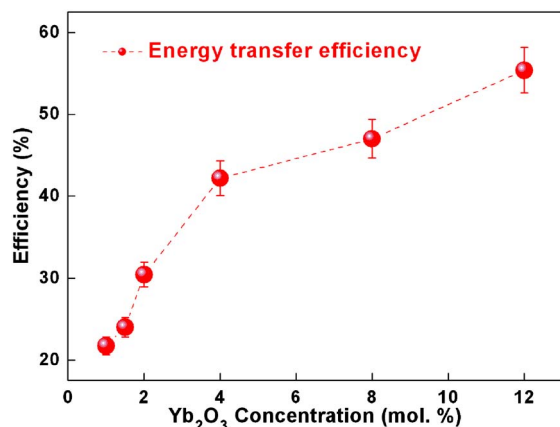


FIG. 8. (Color online) Yb₂O₃ concentration dependent energy transfer efficiency.

and Yb³⁺ as the acceptor. By dividing the mean lifetime of the defect emission of Yb₂O₃ doped glasses over the Yb³⁺-free glass, the transfer efficiency is obtained as a function of Yb₂O₃ concentration,

$$\eta_{\text{ET}} = 1 - \frac{\tau_{m-x\text{Yb}}}{\tau_{m-0\text{Yb}}},$$

where x represents the Yb₂O₃ concentration.

The evaluated Yb₂O₃ concentration dependent transfer efficiency with error bar is shown in Fig. 8. It is seen that the transfer efficiency increases 21% when the concentration of Yb₂O₃ is increased from 1 mol % to 4 mol %, and reaches a maximum value of 56% when 12 mol % Yb₂O₃ is doped.

IV. CONCLUSIONS

In the Yb₂O₃ doped 40SrO-20TiO₂-40SiO₂ glass system, the extraterrestrial solar irradiance of 250–350 nm can be converted into the visible emission of 450–600 nm, and the near-infrared emission of 960–1100 nm where the silicon solar cells exhibit the greatest spectral response. The visible emission with a central wavelength of 520 nm is originated from the silicon-oxygen-related defects in the STS glassy matrix, and the infrared emission of Yb³⁺ ²F_{5/2} → ²F_{7/2} transition is due to the energy transfer from the silicon-oxygen-related defects to Yb³⁺ ions. The occurrence of the energy transfer process was proved by both the steady state and time-resolved emission spectra of Yb³⁺ at low temperatures. The temperature dependent energy transfer rate increases rapidly with increasing temperature, indicating a photon-assistant energy transfer process. The Yb₂O₃ concentration

dependent energy transfer efficiency has the maximum value of 56% for the 12 mol % Yb₂O₃ doped STS glass. These transparent glassy materials may have great potential applications in silicon-based solar cells to enhance their photovoltaic conversion efficiency via spectral modification.

ACKNOWLEDGMENTS

This work was financially supported by National Nature Science Foundation of China (Grant Nos. 50672087, 50802083, and 60778039), National Basic Research Program of China (Grant No. 2006CB806007), and National High Technology Program of China (Grant No. 2006AA03Z304). This work was also supported by the program for Changjiang Scholars and Innovative Research Team in University (Grant No. IRT0651).

- ¹E. Downing, L. Hesselink, J. Ralston, and R. Macfarlane, *Science* **273**, 1185 (1996).
- ²S. F. Zhou, N. Jiang, B. Zhu, H. C. Yang, S. Ye, G. Lakshminarayana, J. H. Hao, and J. R. Qiu, *Adv. Funct. Mater.* **18**, 1 (2008).
- ³B. Zhu, S. M. Zhang, S. F. Zhou, N. Jiang, and J. R. Qiu, *Opt. Lett.* **32**, 653 (2007).
- ⁴G. Blasse and B. C. Grabmaier, *Luminescent Materials* (Springer, Berlin, 1994).
- ⁵S. Ye, B. Zhu, J. X. Chen, J. Luo, and J. R. Qiu, *Appl. Phys. Lett.* **92**, 141112 (2008).
- ⁶S. Ye, B. Zhu, J. X. Chen, J. Luo, G. Lakshminarayana, and J. R. Qiu, *Opt. Express* **16**, 8989 (2008).
- ⁷D. Chen, Y. Wang, Y. Yu, P. Huang, and F. Weng, *Opt. Lett.* **33**, 1884 (2008).
- ⁸A. Shalav, B. S. Richards, and M. A. Green, *Sol. Energy Mater. Sol. Cells* **91**, 829 (2007).
- ⁹T. Trupke, M. A. Green, and P. Würfel, *J. Appl. Phys.* **92**, 1668 (2002).
- ¹⁰P. Vergeer, T. J. H. Vlugt, M. H. F. Kox, M. I. Den Hertog, J. P. J. M. Van der Eerden, and A. Meijerink, *Phys. Rev. B* **71**, 014119 (2005).
- ¹¹Q. Y. Zhang, G. F. Yang, and Z. H. Jiang, *Appl. Phys. Lett.* **91**, 051903 (2007).
- ¹²G. Blasse, *J. Inorg. Nucl. Chem.* **30**, 2283 (1968).
- ¹³Y. Takahashi, K. Kitamura, Y. Benino, T. Fujiwara, and T. Komatsu, *Appl. Phys. Lett.* **86**, 091110 (2005).
- ¹⁴C. Strumpel, M. McCann, G. Beaucarne, V. Arkhipov, A. Slaoui, V. Svrcek, C. del Canizo, and I. Tobias, *Sol. Energy Mater. Sol. Cells* **91**, 238 (2007).
- ¹⁵B. S. Richards, *Sol. Energy Mater. Sol. Cells* **90**, 1189 (2006).
- ¹⁶P. Yang, C. F. Song, M. K. Lu, J. Chang, Y. Z. Wang, Z. X. Yang, G. J. Zhou, Z. P. Ai, D. Xu, and D. L. Yuan, *J. Solid State Chem.* **160**, 272 (2001).
- ¹⁷L. van Pieterse, M. Heeroma, E. de Heer, and A. Meijerink, *J. Lumin.* **91**, 177 (2000).
- ¹⁸J. Sablayrolles, V. Jubera, F. Guillen, and A. Garcia, *Spectrochim. Acta, Part A* **69**, 1010 (2008).
- ¹⁹W. M. Yen and P. M. Selzer, *Laser Spectroscopy of Solids* (Springer Verlag, Berlin, 1981).
- ²⁰W. M. Yen, J. Hegarty, and D. L. Huber, *Proceedings of the International Conference on Lasers '80* (STS Press, Mclean, VA, 1981), Vol. 4, p. 361.